



Published in final edited form as:

*Mech Res Commun.* 2009 January 1; 36(1): 92–103. doi:10.1016/j.mechrescom.2008.08.006.

## Cell Separation by Non-Inertial Force Fields in Microfluidic Systems

Hideaki Tsutsui and Chih-Ming Ho

Mechanical and Aerospace Engineering Department, University of California, Los Angeles, Los Angeles, CA 90095, United States

### Abstract

Cell and microparticle separation in microfluidic systems has recently gained significant attention in sample preparations for biological and chemical studies. Microfluidic separation is typically achieved by applying differential forces on the target particles to guide them into different paths. This paper reviews basic concepts and novel designs of such microfluidic separators with emphasis on the use of non-inertial force fields, including dielectrophoretic force, optical gradient force, magnetic force, and acoustic primary radiation force. Comparisons of separation performances with discussions on physiological effects and instrumentation issues toward point-of-care devices are provided as references for choosing appropriate separation methods for various applications.

### Keywords

cell and microparticle separation; dielectrophoresis; optical gradient force; magnetic force; primary radiation force

### 1. Introduction

During the last fifteen years, development of microfluidic devices (Ho, 2001; Ho and Tai, 1998; Stone et al., 2004) has become a popular research topic because of the advantages they offer over conventional macroscale instruments including lower cost, lower sample and reagent consumption, adaptability for automation, and promise for portable point-of-care devices. Biological, chemical, or medical processes involving complex fluids with embedded particles (e.g., blood) often require preparative separation of particles, cells, or even molecules that are needed for the subsequent procedures. In conventional macroscale separation processes, centrifugation and membrane filtration have been commonly used for many decades, whereas more sophisticated methods such as fluorescent-activated cell sorting (FACS) (Bonner et al., 1972) and magnetically-activated cell separation (MACS) (Miltenyi et al., 1990) were rapidly established as the standard methods for high quality cell and particle separation. During the 1990s, when microelectromechanical systems (MEMS) technology became widely available to researchers and poly(dimethylsiloxane) (PDMS) microchannels (Duffy et al., 1998) were introduced, microfluidics was quickly recognized as a new, exciting scientific field and its applications to chemical and biological processes rapidly expanded. Such technological advance allowed for the miniaturization of filtration devices and the realization of precise channel geometries, leading to separation of cells and particles through a combination of

---

**Publisher's Disclaimer:** This is a PDF file of an unedited manuscript that has been accepted for publication. As a service to our customers we are providing this early version of the manuscript. The manuscript will undergo copyediting, typesetting, and review of the resulting proof before it is published in its final citable form. Please note that during the production process errors may be discovered which could affect the content, and all legal disclaimers that apply to the journal pertain.

microstructures and laminar flow around them. Furthermore, a number of force transducers developed through the last few decades were recently applied to microfluidic devices and used to manipulate microparticles by non-inertial forces including dielectrophoretic (DEP) force, optical gradient force, magnetic force, and acoustic primary radiation force, leading to numerous successful microchip designs for particle and cell separation. Inertial forces such as gravitational force (Huh et al., 2007) and centrifugal force (Madou et al., 2006) can also be used to separate particles. However, due to small differences in density between different subtypes of cells (e.g. red blood cells 1.089–1.100 g/cm<sup>3</sup>, white blood cells 1.055–1.085 g/cm<sup>3</sup> (Sethu et al., 2006)), separation methods based on these forces typically require an extensive separation time or a centrifugal device which severely limits inline integration with other on-chip processes.

Despite growing interests and potential applications of microfluidics-based cell and microparticle separation, there had not been a comprehensive review over various separation methods until very recently (Pamme, 2007), where various continuous flow separation methods for both large molecules and particles ranging from tens of nanometers to micrometers were reviewed. In the present review, we focus on separation methods applicable to cells (on the order of microns), particularly with the use of non-inertial forces. We also address issues such as device performances, physiological effects on cells, and miniaturization toward realization of point-of-care devices.

## 2. Passive separation based on microstructures and laminar flow

Filtration sieves or well-controlled laminar flow can be used to perform separation of particles based on size, shape, and deformability. Without the application of a force field, these approaches prove to be a simple and low-cost method of cell and particle separation.

### 2.1 Filtration sieves

The most straightforward method of cell and particle separation in microfluidic systems is size discrimination by filtration sieves. In the past few years, several groups have developed microfiltration chips with fully integrated fluidic channels and microsieves. For example, an array of microsieves placed perpendicular to the direction of flow was used to fractionate a mixture of cells (Mohamed et al., 2004). This sieving array, consisting of four segments with different pore sizes (2.5 $\mu$ m, 5 $\mu$ m, 10 $\mu$ m, 15 $\mu$ m), successfully trapped red blood cells (RBCs), white blood cells (WBCs) and spiked neuroblastoma, at different segments or in different rows along the flow direction. However, this method suffers from clogging of the microsieves by the cells. One way to alleviate clogging is to use the cross flow channel design, where the liquid flow in the microchannel is continuously extracted to the side channels through micro pores (Fig. 1A). In this design, particles smaller than the pore size are collected into the side channels while particles too large to pass through the pores are continuously flushed away by the mainstream flow. Such cross flow filtration microchips were employed for separation of plasma from whole blood. In one example, the pore height of 0.5 $\mu$ m was small enough to block all the cell population while allowing plasma to flow into the side channels (Crowley and Pizziconi, 2005). In another example of blood filtration, this technique was further improved by the use of external pulsatile pressure to prevent clogging of the channels with blood cells (VanDelinder and Groisman, 2006). In a very recent example, the cross-flow side channels were used for continuous perfusion into the main channel, washing away RBCs and significantly enriching (~4000 fold) WBCs in the main channel (VanDelinder and Groisman, 2007).

## 2.2 Laminar flow

Laminar flow is an intrinsic property of most microfluidic systems due to their small length scale. In a laminar stream, a particle not far from neutral buoyancy (e.g., cells) follows a path which goes through its center of mass. Through careful designing of the flow in a pinched segment or around arrays of posts, such particles can be positioned in the flow so that particles of different sizes will follow different paths, achieving size-based separation.

In a method called “pinched flow fractionation” (Sai et al., 2006; Takagi et al., 2005; Yamada et al., 2004) particles of various sizes were hydrodynamically aligned in a pinched narrow segment and then separated into different trajectories of radially spreading streamlines in a size dependent manner in a diverging laminar flow (Fig. 1B). Another novel approach of using laminar flow is “deterministic lateral displacement” (Huang et al., 2004), where particles’ paths were laterally biased through asymmetric bifurcation of laminar flow around arrayed micron-sized poles depending on the particles size (Fig. 1C). This principle was applied to separate RBCs, WBCs, and platelets (Davis et al., 2006; Zheng et al., 2005a; Zheng et al., 2005b). More recently a subpopulation (CD4<sup>+</sup> T helper lymphocytes) of WBCs was successfully fractionated by increasing the hydrodynamic radius through affinity binding of antibody-coated microbeads (Li et al., 2007).

## 3. Separation with a non-inertial force field

Despite the simplicity of microfluidic separators based on microfiltration and laminar flow profiles, separation purely based on size and shape may not be sufficient for specific applications. For example, it is difficult to separate live cells from dead cells by such methods since their size and shapes may be similar. However, with the compromised cell membrane, dead cells exhibit different dielectric properties from their live counterparts and can be separated by DEP forces. The use of non-inertial forces can also improve separation performance, introduce new separation criteria, and allow more flexible microfluidic channel designs.

The DEP, magnetic, and primary radiation forces (but not optical gradient force) acting on a spherical microparticle of radius  $r$  are listed in Table 1. Derivations of the formulas are beyond the scope of this review and will not be described. Nevertheless, the formulas insightfully tell readers how separation can be implemented by such forces. For example, DEP and magnetic forces are both proportional to the gradient of the field strength squared. This means that besides dielectric and magnetic properties of a particle, a locally focused field (electric field or magnetic field) is necessary for generating a force to manipulate particles. Such localized fields were successfully created by the use of microelectrodes or ferromagnetic microstructures as described in the following sections. The primary radiation force in Table 1 results from acoustic standing waves in the direction of the wave propagation. In a microfluidic system, it is typically generated by an acoustic transducer and a reflector (side walls of the channel) or a pair of acoustic transducers across the microfluidic channel. Finally, the optical gradient force on a particle is well modeled in cases where the particle’s radius,  $r$ , is much smaller (Rayleigh regime) or much larger (Mie regime) than the light wavelength,  $\lambda$ . In the Rayleigh regime a particle behaves as an induced dipole under the inhomogeneous electromagnetic field of light; thus the optical gradient force is analogous to the DEP force (i.e., proportional to both the particle volume and the gradient of the field strength squared). On the other hand, in the Mie regime, the target particle can be considered as a lens, and the optical force, resulting from refraction of focused incident light, can be calculated from simple ray optics. Unfortunately, optical manipulation of cells and microparticles corresponds to an intermediate regime (Lorenz-Mie regime,  $r \sim \lambda$ ) where calculation of the force requires more complete electromagnetic theories, and a simple and intuitive expression of the force is not available.

In the following sections, applications of the DEP, optical gradient, magnetic, and acoustic forces for cell and particle separation are described.

### 3.1 Separation by dielectrophoretic forces

Under a highly non-uniform electric field, polarizable particles (e.g., cells) experience a force in the direction along (positive DEP, pDEP) or against (negative DEP, nDEP) the electric field gradient depending on their dielectric properties. Advancement in microfabrication technology allow for the fabrication of microscale metal electrodes, which are used to generate a strong, non-uniform, time-varying (AC) electric field without the need for applying high potentials. While typical DEP separators use an AC potential small enough to eliminate electroosmosis and gas generation on the microelectrodes, direct current (DC) potential was recently employed (Cummings and Singh, 2003) with insulating posts to generate locally non-uniform electric fields without microelectrodes (DC-iDEP).

There are two common mechanisms of the DEP separation. The first method utilizes differences in the particles' response around a cross-over frequency (Morgan and Green, 2003), where the response switches from pDEP to nDEP, or vice versa. Therefore, by choosing a frequency where one type of particle experiences pDEP, thus attracted to the electrodes, while another type of particle is repelled by nDEP, separation of a binary particle mixture can be achieved. The second strategy is to differentiate particles based on the magnitude of the DEP force. This was initially demonstrated by Gascoyne and coworkers (Wang et al., 2000; Yang et al., 1999, 2000) in a family of separation techniques called field-flow fractionation (Giddings, 1993). In their studies, human cells having different dielectric properties were levitated to different heights in a laminar parabolic flow field by nDEP force generated by interdigitated electrode arrays, and consequently fractionated along the fluidic path. In this section, we will describe continuous flow separation of microparticles and cells by DEP forces. Detailed descriptions on the mechanism and applications of DEP for microscale particle manipulation and separation can be found in other reviews (Gascoyne and Vykoukal, 2002; Gonzalez and Remcho, 2005; Holmes et al., 2003; Hughes, 2002; Voldman, 2006).

**3.1.1 AC dielectrophoresis with microelectrodes**—Recently, a number of groups have developed high-throughput continuous separation systems by exploiting either the sign (Doh and Cho, 2005; Li and Kaler, 2004) or the magnitude (Choi and Park, 2005; Hu et al., 2005; Kralj et al., 2006) of DEP forces to deflect target particles and cells in a laminar flow stream.

Among the examples of the sign-based DEP separation, Li and Kaler (2004) developed a microfluidic cell sorter with an individually biased planar electrode array to generate an isomotive electric field (i.e., constant  $\nabla|\mathbf{E}_{rms}|^2$ ). Under this electric field, where DEP forces were independent of location, viable and nonviable canola cells were separated solely based on their dielectric properties. Similarly, in the microfluidic system developed by Doh and Cho (2005), three planar electrodes laterally diverted live yeast cells away from the central streamline by pDEP, while collecting dead cells into the central streamline by nDEP.

The magnitude-based continuous flow separation was first demonstrated by Choi and Park (2005), where an array of trapezoidal electrodes generated an asymmetric electric field gradient relative to the streamwise direction of the microchannel. Due to balance between the hydrodynamic drag force and the net nDEP force, larger polystyrene microspheres were more deflected than smaller ones in the transverse direction (Fig. 2A). A similar size-based particle separation was demonstrated by nDEP deflection through an asymmetric electric field gradient generated by slanted, narrowly spaced, interdigitated electrodes (Kralj et al., 2006).

Since the DEP force is proportional to the cube of the cell diameter, even slight size variation can result in significant differences in DEP force. Therefore, DEP separation based solely on

cells' dielectric properties is difficult for separating two or more populations of cells with similar sizes. Hu et al. (2005) demonstrated rare cells recovery through the combination of marker-specific labeling of target cells and nDEP deflection. Rare *E. coli* population tagged with dielectric beads, thus experiencing magnified force, was collected into the collection channel by nDEP deflection, while the non-specific *E. coli* population was discharged to the waste channel.

**3.1.2 Direct-current insulator-based dielectrophoresis**—Direct-current insulator-based DEP (DC-iDEP) uses a strong DC potential between the inlet and outlet of a microfluidic channel to generate a bulk flow by electroosmosis, and embedded insulating structures create a non-uniform electric field to induce dielectrophoresis. Without the use of an array of metal microelectrodes, DC-iDEP separation microchips are less prone to fouling, chemically inert, and simpler to operate compared with their AC-DEP counterparts.

The concept of DC-iDEP was introduced as a method of in-flow filtration and concentration of particles by Cummings and Singh (2003). Applying a DC potential voltage across the insulator array induced an electrokinetic flow due to combination of electrophoresis and electroosmosis, while the insulating posts modulated the nearby electric field to form dielectrophoretic traps.

Recently DC-iDEP was employed to achieve continuous separation of microparticles, where local DEP force around an insulating object, such as an oil droplet (Barbulovic-Nad et al., 2006) or a PDMS block (Kang et al., 2006), differentiated trajectories of microparticles in a size-dependent manner (Fig. 2B,C).

### 3.2. Separation by optical forces

A focused beam of light can directly manipulate objects of size ranging from the nano to micro scales. For a dielectric particle whose diameter is substantially smaller than the wavelength  $\lambda$  of light, the particle is considered as an induced dipole under the electromagnetic field of the incident light. Subsequently, the particle whose permittivity is larger than the surrounding medium is pulled toward the focal point of the light beam, where the electromagnetic field is strongest. For a particle much larger than  $\lambda$ , the trapping force is interpreted as a result of momentum exchange between the refracted light and the dielectric particle. The optical separation of microparticles combines a laminar flow stream and various forms of focused laser beams ranging from a single spot (termed an optical potential well), arrays of potential wells, to interconnected wells (termed optical lattices). Unlike other forces (DEP, magnetic, or hydrodynamic forces) of which online reconfiguration is limited, optical forces can be dynamically tuned in time and space. Detailed overview of optical micromanipulation was recently documented by Grier (2003), Neuman and Block (2004), and Dholakia and coworkers (2006 (2008)).

**3.2.1 Passive separation with optical potential landscapes**—Various forms of optical potential landscapes, including a line optical tweezers formed by a cylindrical lens (Cheong et al., 2006) and arrays of optical potential wells made by multi-beam interference (Ladavac et al., 2004; MacDonald et al., 2004; MacDonald et al., 2003) or a microlens array (Sun et al., 2006) can be used in combination with laminar flow to separate particles in microfluidic systems. In such separation systems, particles with higher optical affinity (e.g., larger refractive index, and size) experience optical trapping forces large enough to be diverted from the flow direction, while the path of the other particles remain almost unchanged. For example, a body-centered tetragonal (BCT) optical lattice made by a five-beam interference pattern was used to separate polymer and silica microspheres, protein microcapsules, and mouse RBCs and WBCs based on difference in refractive indices, size, and shape, respectively

(MacDonald et al., 2004; MacDonald et al., 2003). Particles with a higher affinity for the optical potential were deflected 45 degrees from the flow direction along the diagonal linking of intensity maxima of the BCT lattice, while particles with a lower affinity stayed along the flow direction (Fig. 3A).

While the above particle separation technique based on optical potential wells was only demonstrated on bidisperse particle mixtures, fractionation of polydisperse particle mixtures can be achieved through careful designing of optical potential landscapes. Recently, continuous flow separation of silica spheres of four different sizes (2.3, 3.0, 5.17, and 6.84 $\mu\text{m}$ ) was demonstrated (Milne et al., 2007). In this study, temporally modulated raster scanning of a laser beam was used to create two diagonal optical guides, forming a “V” shape (Fig. 3B inset). All the particles flowing from right to left were trapped by the right arm of the guide, then moved over to and carried along the left guide. Along the left arm, consisting of discrete segments with decreasing light intensities, the trapped particles were released into the flow in a size-increasing order as the optical gradient force was overcome by Stokes drag force, resulting in lateral fractionation of particles (Fig. 3B).

**3.2.2 Microfluidic fluorescent activated cell sorters**—Microscale fluorescent activated cell sorting (FACS) combines branching laminar flow and optical force switching to select target cells (Applegate et al., 2004; Applegate et al., 2006; Wang et al., 2005). In the system of Applegate et al. (2004; 2006), an optical bar trap was focused across the branching laminar flow so that non-fluorescent particles were trapped and completely translated along the optical trap and then released into a collection channel. Upon fluorescent particles' entering the trap, a computer-controlled detector-shutter system blocked the optical trapping beam. Consequently, fluorescent particles were released into a stream leading to another collection channel. Wang et al. (2005) used a similar system but with an acousto-optic modulator enabling rapid switching of the optical force sorter, achieving a separation speed up to 100 cells per second (Fig. 3C).

**3.2.3 Light-activated dielectrophoresis**—Recently, a light-activated dielectrophoresis device called optoelectronic tweezers (OET) was proposed by Chiou et al. (2005). The OET fluidic device typically consists of a blank indium tin oxide-coated glass (ITO glass) top plate and a photoconductive layer-coated ITO glass bottom plate, with an AC voltage applied between the plates. Illumination of light pattern from light-emitting diode and digital micromirror spatial light modulator creates virtual electrodes in the photoconductive layer, resulting in a non-uniform electric field and enabling light-guided DEP manipulation. Although the trapping energy is supplied by the AC-biased voltage, OET allows for both flexibility of light pattern formation and versatility of DEP manipulation (Dholakia, 2005). Besides the flow-free separation of bidisperse polystyrene microbeads and live/dead B cells demonstrated by Chiou et al. (2005), OET can be readily used to perform the continuous-flow AC-DEP particle separation described in section 3.1.1.

### 3.3 Separation by magnetic forces

The motion of magnetic particles and magnetically labeled biological objects can be manipulated by magnetic forces in microfluidic devices. Magnetic separation of cells typically requires labeling of magnetic beads; the only cells that naturally demonstrate magnetic susceptibility sufficient for magnetic manipulation are RBCs (Han and Frazier, 2006) and magnetotactic bacteria (Schuler and Frankel, 1999). Magnetic fields can extend to relatively long distances and manipulate many magnetic targets simultaneously in wide range of pH, ionic concentrations, and temperatures required for chemical and biological processing in microfluidic systems. Principles of magnetic operations and various applications in microfluidic systems were recently reviewed by Pamme (2006).

**3.3.1 Continuous flow separation of magnetically tagged cells**—Non-magnetic cells can be labeled with magnetic particles through antigen-antibody interactions and sorted into specific subpopulations. In continuous flow magnetic separation, magnetic forces are applied perpendicular to the flow direction to divert particles into different trajectories. One of the challenges in achieving magnetic separation in microfluidic systems is to generate a locally strong magnetic field gradient; as indicated in Eq. 2 in Table 1, a strong but homogeneous magnetic flux cannot exert a magnetic force on particles.

Microfabrication technology allows for the fabrication and integration of microscale magnetic materials on microfluidic chips. These ferromagnetic microstructures, upon magnetization by an external field, will create a strong magnetic field gradient inside the microfluidic channel. For example, ferromagnetic (nickel) stripes fabricated on a silicon chip were used as a magnetic trap and deflector to separate magnetically labeled WBCs from a continuous stream of blood cells (Inglis et al., 2004). In another example, a NiFe microcomb structure fabricated by electroplating was used to generate a strong magnetic field gradient across the microchannel for the purpose of extracting magnetically tagged *E. coli* from a flow containing RBCs (Fig. 4A) (Xia et al., 2006). Fabrication processes employed in the above studies, including sputter deposition, chemical mechanical planarization, and electroplating are time consuming and require expertise. Recently, a simpler method was demonstrated where a ferromagnetic microstructure was created by the injection of nickel microparticles into a microchannel adjacent to the separation channel (Lin et al., 2007).

All of the above continuous flow magnetic separation techniques were designed and demonstrated for binary separation of target magnetic particles (or magnetically tagged cells) from non-magnetic ones. In a method called free-flow magnetophoresis, however, the same magnetic deflection was combined with an array of laminar flow outlets to differentially separate magnetic particles based on the sizes and susceptibilities (Fig. 4B) (Pamme et al., 2006;Pamme and Manz, 2004).

### 3.4 Separation by acoustic forces

In an ultrasonic standing wave field, particles experience acoustic radiation forces. These forces can be divided into the primary radiation force, originating from fluctuations of the molecules of the medium, and the secondary interparticle force (Bjerknes force), caused by scattering of the incident acoustic waves. Since the primary radiation force is usually orders of magnitude larger than the secondary forces, acoustic separation devices generally utilize the primary radiation force. In an ultrasonic standing wave field, the primary radiation force moves particles toward the pressure nodes or antinodes depending on the acoustic contrast factor ( $\phi$  in Eq. 3 in Table 1), a function of density and compressibility of the particles and the medium. Therefore, particles with different acoustic properties can be accumulated to different positions (the nodes and antinodes) and collected separately with help of a laminar flow in a microfluidic ultrasound separation device. Reviews on principles of ultrasound manipulations and various applications in microscale are available elsewhere (de Castro and Priego-Capote, 2007;Laurell et al., 2007;Wiklund and Hertz, 2006).

**3.4.1 Continuous flow separation of mixed particles**—Acoustic separation of a mixed particle population can be categorized into two types: binary separations based on the sign of  $\phi$ , and differential separations based on the magnitude of the primary radiation force (i.e., size of particles and magnitudes of  $\phi$ ). A typical example of the first separation type is cleaning of RBCs (positive  $\phi$ ) contaminated with lipid microemboli (negative  $\phi$ ) demonstrated by Laurell and coworkers (Nilsson et al., 2004; Petersson et al., 2004, 2005). In the trifurcating silicon microchannel, an acoustic standing wave was generated by a single piezoceramic transducer attached on the back side. RBCs were focused into the pressure nodal plane along the center

of the channel and lipids were drawn into the antinodal planes near the side walls, and subsequently collected through different outlets (Fig. 5A, B).

Although the sign-based binary separation approach is relatively simple and highly efficient, its application is limited to binary mixtures of positive and negative  $\phi$  particles. Typically, most cell types have a positive  $\phi$  due to their higher density and lower compressibility than that of the surrounding medium. Hence, one has to utilize the difference of the force magnitude in order to sort out heterogeneous cell populations by size and other properties. Such size-based separation of cells and particles in a microfluidic system was demonstrated by several groups (Kapishnikov et al., 2006; Kumar et al., 2005; Laurell et al., 2007). The primary radiation force scales with the cube of the particle size and the Stokes drag force scales with the particle's diameter, resulting in the particle's net speed of movement toward the pressure nodal plane scaling with the square of its size (Kumar et al., 2005). Thus in combination with laminar flow, particles can be separated in a size-dependent and continuous manner (free flow acoustophoresis: Fig. 5C). For example, Kapishnikov et al. (2006) successfully extracted the larger particles from a stream of mixture (2.5 $\mu\text{m}$  and 10 $\mu\text{m}$  polyamide particles) into an adjacent carrier stream. In this PDMS device, a pair of piezoceramic transducers were used to create the pressure nodal plane in the carrier stream and anti-nodal planes in the mixture stream. Although both particle types experienced the force toward the pressure nodal plane, the size dependency resulted in extraction of only 10 $\mu\text{m}$  particles into the carrier stream. Recently, free flow acoustophoresis of a mixture of four particle sizes (2, 5, 8, and 10 $\mu\text{m}$ ) and a mixture of RBCs, platelets, and WBCs were successfully demonstrated in separate experiments (Pettersson et al., 2007). The latter experiment required addition of cesium chloride into the suspending medium in order to increase the medium's density and consequently contrast relative acoustic properties of RBCs and platelets.

#### 4. Comparison of separation methods

Different categories of microfluidic particle separation are listed for comparison purposes in Table 2. Resolution, efficiency and throughput are selected from the recent literature as indicated in the footnote. As a cautionary note, the presented data should be used as an estimation of the performances of each separation mechanism as of the present and should not be viewed as the ultimate performances of the devices; further improvements from novel ideas and optimization of the devices are yet to emerge in the near future. Table 2 shows that both separation resolution and efficiency are similar across the board. It should be noted, however, that separation of submicron-sized particles will be increasingly difficult with the non-inertial forces since such forces scale with the particle volume (Table 1), while opposing Stokes drag is proportional to the diameter. On the other hand, laminar flow methods have demonstrated successful separation of submicron particles (pinched-flow fractionation)(Sai et al., 2006) and even DNA fragments (deterministic lateral displacement)(Huang et al., 2004). However, performance of these methods is extremely sensitive to quality of the laminar flow including particle alignment by the sheath flow. Such requirements constrain separation to be performed at relatively low sample concentration and flow rates, resulting in lower throughput than the non-inertial force methods. On the other hand, the non-inertial force methods allow adjustment of the trapping forces independent of the flow speed and can handle a significantly larger flux of particles.

Another important point of discussion is the physiological effects of each separation method on cells. The filtration and laminar flow approaches, with a channel consisting of narrow pores or arrays of obstacles, tend to suffer from clogging and shear stress leading to rupture of the cells (VanDelinder and Groisman, 2006). Especially in pinched-flow fractionation by Takagi et al. (2005), where the flow rate  $Q$  is 1020 $\mu\text{l/h}$  through the rectangular pinched section ( $w \times d = 20\mu\text{m} \times 20\mu\text{m}$ ), average wall shear stress in the pinched section is, assuming a fully



developed Newtonian flow, estimated to exceed 200Pa by the following analytical solution (White, 1991),

$$\bar{\tau}_w = \frac{6\mu Q}{w^2(w+d) \left[ 1 - \frac{192w}{\pi^5 d} \sum_{k=1,3,5,\dots}^{\infty} \frac{\tanh(k\pi b/2w)}{k^5} \right]} \quad (4)$$

Although apparent hemolysis was not observed, probably because of very short exposure time (~ ms), such high wall shear stress was above the onset value (~100Pa) of mammalian cell lysis previously reported (Ma et al., 2002). Of course, shear stress can be reduced by using lower flow rate, however, at the expense of lower throughput. From Eq. 4 the average wall shear stress of the non-inertial force methods listed in Table 2 were estimated to be on the order of 0.01 to 1Pa.

Although non-inertial forces allow for high-throughput cell separation without suffering from high shear stress, the use of specific force fields could also damage or influence the cells. First, DEP manipulation with microelectrode could impose problems of Joule heating and electric field exposure. Joule heating, however, is typically not significant due to the large surface-to-volume ratio of microfluidic systems which allows for fast dissipation of heat out of the system. On the other hand, the electric field could affect endogenous transmembrane voltages and influence membrane-bound components of the cells. Such electric field-related effects are usually minimized by choosing operation conditions to which cells are less sensitive (> MHz, < 10kV/m) (Voldman, 2006).

Typically, high power density of optical traps (~10<sup>7</sup> W/cm<sup>2</sup>) is known to affect viability (Liu et al., 1996), clonal growth (Liang et al., 1996), and motility (Neuman et al., 1999) of cells and damage DNA (Mohanty et al., 2002). Although the optical separation methods reviewed in this paper use power density of a similar level, the retention time (the duration for which cells were optically trapped) is on the order of milliseconds to seconds compared to tens to hundreds of seconds in the above studies. For example, study on cell stress gene expressions by Wang et al. (2005) did not show any significant increase in the examined stress markers. Likewise, physiological effects of optical manipulation in the continuous flow cell separation seem to be minimal.

Magnetic cell separation is generally considered to be non-lethal to cells and is widely used in various forms (Safarik and Safarikova, 1999). Microfluidic magnetic separation typically utilizes a magnetic flux density in the range of 0.001~1T, and such magnetic fields are known to induce various physiological effects in a progressive manner during several hours of exposure (Dini and Abbro, 2005). Since target cells typically experiences magnetic forces for less than 1 second in the devices described in this review, gross effects of the magnetic field in such devices seem to be minimal.

Acoustic manipulation within a microfluidic channel could result in temperature increase of up to 10°C due to dissipation of the acoustic energy into thermal energy (Evander et al., 2007). Therefore, care must be taken to keep the operation temperature (after the temperature rise) below the physiological temperature of cells in order to avoid a heat shock response (Lindquist, 1986) or more adverse effects on cells. One approach could be to prepare the cell suspension at a lower temperature in order to compensate for the heat generated by the acoustic energy. In the study by Evander et al. (2007), where the temperature was controlled not to exceed the physiological temperature, no perceptible damage to the cells (growth of yeasts and

viability of rat neural stem cells) due to the acoustic manipulation was observed, indicating that acoustic cell separation can be performed without significantly affecting cells' physiology.

It is important to note that any cell manipulation method will induce physiological effects on live cells including well-established methods such as FACS and MACS. For example, in the study of cell membrane physiology by Seidl et al. (1999), FACS processing was found to lower the membrane integrity (i.e., cell viability) of normal human skin fibroblast cells N1 and human breast carcinoma cells BT474 down to 75–80% compared to >90% of the control population. In the same study, MACS processing was found to cause significant membrane hyperpolarization in both BT474 and N1 cells.

Finally, the portability of each device needs to be briefly discussed because this is an important aspect in the development of portable point-of-care devices. Both cross flow filtration and laminar flow methods are considered to be highly portable as they only require fluidic pumps (or other pressure sources) besides the microfluidic separator chip. Magnetic method falls into the same category as it only needs a permanent magnet in addition to the pumps and separation chip. DEP and acoustic approaches both require a power supply, putting them in the portable category; such power supply units can be miniaturized relatively easily. Among the listed methods, the optical approach is considered to be least portable since this method requires a rather bulky laser optic system (e.g., a high-power laser source(s), a detector(s), an acousto-optic deflector(s), various lenses and mirrors, etc.), which cannot be easily miniaturized without significantly compromising the performance.

## 5. Conclusion

Various strategies of microfluidic cell and particle separation with the use of the non-inertial forces including dielectrophoretic, optical, magnetic, and acoustic forces were reviewed. Each approach proved effective in separating binary mixtures of microscale particles and even demonstrated successful separation of polydisperse mixtures through novel designs. Deciding which method to use should be based on the needs of the application including separation criteria, resolution, efficiency, and throughput, as well as physiological effects. Although physiological effects due to non-inertial forces in microfluidic cell separation might not be more harmful than in any other cell manipulation method, further investigation should be performed to elucidate the mechanism and significance of such forces specifically under microfluidic separation conditions. Meanwhile, users can perform a set of control experiments to identify operation conditions under which certain physiological effects are in a tolerable range.

So far, most demonstrations of the described separation methods were proof of concept with user-defined mixtures (e.g., binary mixture of polystyrene particles) or biological samples conditioned prior to the experiment. Therefore, further characterization and optimization will be required before these separation methods can be used for clinical applications. Another challenge is in-line integration with pre- and post-separation processes on a single chip device and its miniaturization toward portable point-of-care systems. With recent development of various microfabricated on-chip pumps and valves (Dittrich et al., 2006), such developments are certainly feasible. Finally, combinations of multiple forces can offer opportunities to achieve highly specific and efficient separation of complex mixtures of cell populations. For example, DEP-based deflectors and an acoustic transducer were recently integrated to demonstrate simultaneous handling of individual particles in a high-throughput manner (Wiklund et al., 2006). Such efforts could also lead to discoveries of new identities of cell subtypes characterized by a set of intrinsic properties including size, permittivity, refractive index, susceptibility, density and compressibility.

## Acknowledgments

The authors would like to thank Charlotte Kwong, Peter Lillehoj, Dr. Martin Ma, Jeong Wong, Tak Sing Wong, and Edmond Yu for their helpful comments. This publication is supported by the National Institute of Health through the NIH Roadmap for Nanomedicine (PN2 EY018228).

## References

- Applegate RW, Squier J, Vestad T, Oakey J, Marr DWM. Optical trapping, manipulation, and sorting of cells and colloids in microfluidic systems with diode laser bars. *Optics Express* 2004;12:4390–4398. [PubMed: 19483988]
- Applegate RW, Squier J, Vestad T, Oakey J, Marr DWM, Bado P, Dugan MA, Said AA. Microfluidic sorting system based on optical waveguide integration and diode laser bar trapping. *Lab on a Chip* 2006;6:422–426. [PubMed: 16511626]
- Barbulovic-Nad I, Xuan XC, Lee JSH, Li DQ. DC-dielectrophoretic separation of microparticles using an oil droplet obstacle. *Lab on a Chip* 2006;6:274–279. [PubMed: 16450038]
- Bonner WA, Sweet RG, Hulett HR, Herzenbe La. Fluorescence Activated Cell Sorting. *Review of Scientific Instruments* 1972;43:404–409. [PubMed: 5013444]
- Cheong FC, Sow CH, Wee ATS, Shao P, Bettiol AA, van Kan JA, Watt F. Optical travelator: transport and dynamic sorting of colloidal microspheres with an asymmetrical line optical tweezers. *Applied Physics B-Lasers and Optics* 2006;83:121–125.
- Chiou PY, Ohta AT, Wu MC. Massively parallel manipulation of single cells and microparticles using optical images. *Nature* 2005;436:370–372. [PubMed: 16034413]
- Choi S, Park JK. Microfluidic system for dielectrophoretic separation based on a trapezoidal electrode array. *Lab on a Chip* 2005;5:1161–1167. [PubMed: 16175274]
- Crowley TA, Pizziconi V. Isolation of plasma from whole blood using planar microfilters for lab-on-a-chip applications. *Lab on a Chip* 2005;5:922–929. [PubMed: 16100575]
- Cummings EB, Singh AK. Dielectrophoresis in microchips containing arrays of insulating posts: Theoretical and experimental results. *Analytical Chemistry* 2003;75:4724–4731. [PubMed: 14674447]
- Davis JA, Inglis DW, Morton KJ, Lawrence DA, Huang LR, Chou SY, Sturm JC, Austin RH. Deterministic hydrodynamics: Taking blood apart. *Proceedings of the National Academy of Sciences of the United States of America* 2006;103:14779–14784. [PubMed: 17001005]
- de Castro MDL, Priego-Capote F. Lesser known ultrasound-assisted heterogeneous sample-preparation procedures. *Trac-Trends in Analytical Chemistry* 2007;26:154–162.
- Dholakia K. Micromanipulation - Optoelectronic tweezers. *Nature Materials* 2005;4:579–580.
- Dholakia K, Reece P. Optical micromanipulation takes hold. *Nano Today* 2006;1:18–27.
- Dholakia K, Reece P, Gu M. Optical micromanipulation. *Chemical Society Reviews* 2008;37:42–55. [PubMed: 18197332]
- Dini L, Abbro L. Bioeffects of moderate-intensity static magnetic fields on cell cultures. *Micron* 2005;36:195–217. [PubMed: 15725590]
- Dittrich PS, Tachikawa K, Manz A. Micro total analysis systems. Latest advancements and trends. *Analytical Chemistry* 2006;78:3887–3907. [PubMed: 16771530]
- Doh I, Cho YH. A continuous cell separation chip using hydrodynamic dielectrophoresis (DEP) process. *Sensors and Actuators a-Physical* 2005;121:59–65.
- Duffy DC, McDonald JC, Schueller OJA, Whitesides GM. Rapid prototyping of microfluidic systems in poly(dimethylsiloxane). *Analytical Chemistry* 1998;70:4974–4984.
- Evander M, Johansson L, Lilliehorn T, Piskur J, Lindvall M, Johansson S, Almqvist M, Laurell T, Nilsson J. Noninvasive acoustic cell trapping in a microfluidic perfusion system for online bioassays. *Analytical Chemistry* 2007;79:2984–2991. [PubMed: 17313183]
- Gascoyne PRC, Vykoukal J. Particle separation by dielectrophoresis. *Electrophoresis* 2002;23:1973–1983. [PubMed: 12210248]
- Giddings JC. Field-Flow Fractionation - Analysis of Macromolecular, Colloidal, and Particulate Materials. *Science* 1993;260:1456–1465. [PubMed: 8502990]

- Gonzalez CF, Remcho VT. Harnessing dielectric forces for separations of cells, fine particles and macromolecules. *Journal of Chromatography A* 2005;1079:59–68. [PubMed: 16038291]
- Grier DG. A revolution in optical manipulation. *Nature* 2003;424:810–816. [PubMed: 12917694]
- Han KH, Frazier AB. Paramagnetic capture mode magnetophoretic microseparator for blood cells. *IEE Proceedings-Nanobiotechnology* 2006;153:67–73. [PubMed: 16948490]
- Hatch GP, Stelter RE. Magnetic design considerations for devices and particles used for biological high-gradient magnetic separation (HGMS) systems. *Journal of Magnetism and Magnetic Materials* 2001;225:262–276.
- Ho, CM. Fluidics-the link between micro and nano sciences and technologies, *Micro Electro Mechanical Systems, 2001. MEMS 2001; The 14th IEEE International Conference; 2001.* p. 375-384.
- Ho CM, Tai YC. Micro-electro-mechanical-systems (MEMS) and fluid flows. *Annual Review of Fluid Mechanics* 1998;30:579–612.
- Holmes D, Green NG, Morgan H. Microdevices for dielectrophoretic flow-through cell separation. *Ieee Engineering in Medicine and Biology Magazine* 2003;22:85–90. [PubMed: 15007995]
- Hu XY, Bessette PH, Qian JR, Meinhart CD, Daugherty PS, Soh HT. Marker-specific sorting of rare cells using dielectrophoresis. *Proc Natl Acad Sci U S A* 2005;102:15757–15761. [PubMed: 16236724]
- Huang LR, Cox EC, Austin RH, Sturm JC. Continuous particle separation through deterministic lateral displacement. *Science* 2004;304:987–990. [PubMed: 15143275]
- Hughes MP. Strategies for dielectrophoretic separation in laboratory-on-a-chip systems. *Electrophoresis* 2002;23:2569–2582. [PubMed: 12210160]
- Huh D, Bahng JH, Ling YB, Wei HH, Kripfgans OD, Fowlkes JB, Grotberg JB, Takayama S. Gravity-driven microfluidic particle sorting device with hydrodynamic separation amplification. *Analytical Chemistry* 2007;79:1369–1376. [PubMed: 17297936]
- Inglis DW, Riehn R, Austin RH, Sturm JC. Continuous microfluidic immunomagnetic cell separation. *Applied Physics Letters* 2004;85:5093–5095.
- Jones, TB. *Electromechanics of Particles*. Cambridge University Press; New York: 1995.
- Kang KH, Kang YJ, Xuan XC, Li DQ. Continuous separation of microparticles by size with direct current-dielectrophoresis. *Electrophoresis* 2006;27:694–702. [PubMed: 16385598]
- Kapishnikov S, Kantsler V, Steinberg V. Continuous particle size separation and size sorting using ultrasound in a microchannel. *Journal of Statistical Mechanics-Theory and Experiment*. 2006
- Kralj JG, Lis MTW, Schmidt MA, Jensen KF. Continuous dielectrophoretic size-based particle sorting. *Analytical Chemistry* 2006;78:5019–5025. [PubMed: 16841925]
- Kumar M, Feke DL, Belovich JM. Fractionation of cell mixtures using acoustic and laminar flow fields. *Biotechnology and Bioengineering* 2005;89:129–137. [PubMed: 15593262]
- Ladavac K, Kasza K, Grier DG. Sorting mesoscopic objects with periodic potential landscapes: Optical fractionation. *Physical Review E* 2004;70:010901.
- Laurell T, Petersson F, Nilsson A. Chip integrated strategies for acoustic separation and manipulation of cells and particles. *Chemical Society Reviews* 2007;36:492–506. [PubMed: 17325788]
- Li, N.; Kamei, DT.; Ho, CM. On-chip continuous blood cell subtype separation by deterministic lateral displacement. *Proceedings of the 2nd IEEE International Conference on Nano/Micro Engineered and Molecular Systems; Bangkok, Thailand. 2007.* p. 932-936.
- Li Y, Kaler KVIS. Dielectrophoretic fluidic cell fractionation system. *Analytica Chimica Acta* 2004;507:151–161.
- Liang H, Vu KT, Krishnan P, Trang TC, Shin D, Kimel S, Berns MW. Wavelength dependence of cell cloning efficiency after optical trapping. *Biophysical Journal* 1996;70:1529–1533. [PubMed: 8785310]
- Lin YA, Wong TS, Bhardwaj U, Chen JM, McCabe E, Ho CM. Formation of high electromagnetic gradients through a particle-based microfluidic approach. *Journal of Micromechanics and Microengineering* 2007;17:1299–1306.
- Lindquist S. The Heat-Shock Response. *Annual Review of Biochemistry* 1986;55:1151–1191.

- Liu Y, Cheng DK, Sonek GJ, Berns MW, Chapman CF, Tromberg BJ. Evidence for Localized Cell Heating Induced by Infrared Optical Tweezers. *Biophysical Journal* 1995;68:2137–2144. [PubMed: 7612858]
- Liu Y, Sonek GJ, Berns MW, Tromberg BJ. Physiological monitoring of optically trapped cells: Assessing the effects of confinement by 1064-nm laser tweezers using microfluorometry. *Biophysical Journal* 1996;71:2158–2167. [PubMed: 8889192]
- Ma NN, Koelling KW, Chalmers JJ. Fabrication and use of a transient contractional flow device to quantify the sensitivity of mammalian and insect cells to hydrodynamic forces. *Biotechnology and Bioengineering* 2002;80:428–437. [PubMed: 12325151]
- MacDonald MP, Neale S, Paterson L, Richies A, Dholakia K, Spalding GC. Cell cytometry with a light touch: Sorting microscopic matter with an optical lattice. *Journal of Biological Regulators and Homeostatic Agents* 2004;18:200–205. [PubMed: 15471228]
- MacDonald MP, Spalding GC, Dholakia K. Microfluidic sorting in an optical lattice. *Nature* 2003;426:421–424. [PubMed: 14647376]
- Madou M, Zoval J, Jia G, Kido H, Kim J, Kim N. LAB ON A CD. *Annual Review of Biomedical Engineering* 2006;8:601–628.
- Milne G, Rhodes D, MacDonald M, Dholakia K. Fractionation of polydisperse colloid with acousto-optically generated potential energy landscapes. *Optics Letters* 2007;32:1144–1146. [PubMed: 17410263]
- Miltenyi S, Muller W, Weichel W, Radbruch A. High-Gradient Magnetic Cell-Separation with Macs. *Cytometry* 1990;11:231–238. [PubMed: 1690625]
- Mohamed H, McCurdy LD, Szarowski DH, Duva S, Turner JN, Caggana M. Development of a rare cell fractionation device: Application for cancer detection. *Ieee Transactions on Nanobioscience* 2004;3:251–256. [PubMed: 15631136]
- Mohanty SK, Rapp A, Monajembashi S, Gupta PK, Greulich KO. Comet assay measurements of DNA damage in cells by laser microbeams and trapping beams with wavelengths spanning a range of 308 nm to 1064 nm. *Radiation Research* 2002;157:378–385. [PubMed: 11893239]
- Morgan, H.; Green, NG. *AC Electrokinetics: colloids and nanoparticles*. Research Studies Press; Baldock, England: 2003.
- Neuman KC, Block SM. Optical trapping. *Review of Scientific Instruments* 2004;75:2787–2809. [PubMed: 16878180]
- Neuman KC, Chadd EH, Liou GF, Bergman K, Block SM. Characterization of photodamage to *Escherichia coli* in optical traps. *Biophysical Journal* 1999;77:2856–2863. [PubMed: 10545383]
- Nilsson A, Petersson F, Jonsson H, Laurell T. Acoustic control of suspended particles in micro fluidic chips. *Lab on a Chip* 2004;4:131–135. [PubMed: 15052353]
- Pamme N. Magnetism and microfluidics. *Lab on a Chip* 2006;6:24–38. [PubMed: 16372066]
- Pamme N. Continuous flow separations in microfluidic devices. *Lab on a Chip* 2007;7:1644–1659. [PubMed: 18030382]
- Pamme N, Eijkel JCT, Manz A. On-chip free-flow magnetophoresis: Separation and detection of mixtures of magnetic particles in continuous flow. *Journal of Magnetism and Magnetic Materials* 2006;307:237–244.
- Pamme N, Manz A. On-chip free-flow magnetophoresis: Continuous flow separation of magnetic particles and agglomerates. *Analytical Chemistry* 2004;76:7250–7256. [PubMed: 15595866]
- Peterman EJG, Gittes F, Schmidt CF. Laser-induced heating in optical traps. *Biophysical Journal* 2003;84:1308–1316. [PubMed: 12547811]
- Petersson F, Aberg L, Sward-Nilsson AM, Laurell T. Free flow acoustophoresis: Microfluidic-based mode of particle and cell separation. *Analytical Chemistry* 2007;79:5117–5123. [PubMed: 17569501]
- Petersson F, Nilsson A, Holm C, Jonsson H, Laurell T. Separation of lipids from blood utilizing ultrasonic standing waves in microfluidic channels. *Analyst* 2004;129:938–943. [PubMed: 15457327]
- Petersson F, Nilsson A, Holm C, Jonsson H, Laurell T. Continuous separation of lipid particles from erythrocytes by means of laminar flow and acoustic standing wave forces. *Lab on a Chip* 2005;5:20–22. [PubMed: 15616735]

- Safarik I, Safarikova M. Use of magnetic techniques for the isolation of cells. *Journal of Chromatography B* 1999;722:33–53.
- Sai Y, Yamada M, Yasuda M, Seki M. Continuous separation of particles using a microfluidic device equipped with flow rate control valves. *Journal of Chromatography A* 2006;1127:214–220. [PubMed: 16890945]
- Schuler D, Frankel RB. Bacterial magnetosomes: microbiology, biomineralization and biotechnological applications. *Applied Microbiology and Biotechnology* 1999;52:464–473. [PubMed: 10570793]
- Seidl J, Knuechel R, Kunz-Schughart LA. Evaluation of membrane physiology following fluorescence activated or magnetic cell separation. *Cytometry* 1999;36:102–111. [PubMed: 10554157]
- Sethu P, Sin A, Toner M. Microfluidic diffusive filter for apheresis (leukapheresis). *Lab on a Chip* 2006;6:83–89. [PubMed: 16372073]
- Stone HA, Stroock AD, Ajdari A. Engineering flows in small devices: Microfluidics toward a lab-on-a-chip. *Annual Review of Fluid Mechanics* 2004;36:381–411.
- Sun YY, Ong LS, Yuan XC. Composite-microlens-array-enabled microfluidic sorting. *Applied Physics Letters* 2006;89:141108.
- Takagi J, Yamada M, Yasuda M, Seki M. Continuous particle separation in a microchannel having asymmetrically arranged multiple branches. *Lab on a Chip* 2005;5:778–784. [PubMed: 15970972]
- VanDelinder V, Groisman A. Separation of plasma from whole human blood in a continuous cross-flow in a molded microfluidic device. *Analytical Chemistry* 2006;78:3765–3771. [PubMed: 16737235]
- VanDelinder V, Groisman A. Perfusion in microfluidic cross-flow: Separation of white blood cells from whole blood and exchange of medium in a continuous flow. *Analytical Chemistry* 2007;79:2023–2030. [PubMed: 17249639]
- Voldman J. Electrical forces for microscale cell manipulation. *Annual Review of Biomedical Engineering* 2006;8:425–454.
- Wang MM, Tu E, Raymond DE, Yang JM, Zhang HC, Hagen N, Dees B, Mercer EM, Forster AH, Kariv I, Marchand PJ, Butler WF. Microfluidic sorting of mammalian cells by optical force switching. *Nature Biotechnology* 2005;23:83–87.
- Wang XB, Yang J, Huang Y, Vykoukal J, Becker FF, Gascoyne PRC. Cell separation by dielectrophoretic field-flow-fractionation. *Analytical Chemistry* 2000;72:832–839. [PubMed: 10701270]
- White, FM. *Viscous Fluid Flow*. Vol. 2. McGraw-Hill; New York: 1991.
- Wiklund M, Gunther C, Lemor R, Jager M, Fuhr G, Hertz HM. Ultrasonic standing wave manipulation technology integrated into a dielectrophoretic chip. *Lab on a Chip* 2006;6:1537–1544. [PubMed: 17203158]
- Wiklund M, Hertz HM. Ultrasonic enhancement of bead-based bioaffinity assays. *Lab on a Chip* 2006;6:1279–1292. [PubMed: 17102841]
- Xia N, Hunt TP, Mayers BT, Alsberg E, Whitesides GM, Westervelt RM, Ingber DE. Combined microfluidic-micromagnetic separation of living cells in continuous flow. *Biomedical Microdevices* 2006;8:299–308. [PubMed: 17003962]
- Yamada M, Nakashima M, Seki M. Pinched flow fractionation: Continuous size separation of particles utilizing a laminar flow profile in a pinched microchannel. *Analytical Chemistry* 2004;76:5465–5471. [PubMed: 15362908]
- Yang J, Huang Y, Wang XB, Becker FF, Gascoyne PRC. Cell separation on microfabricated electrodes using dielectrophoretic/gravitational field flow fractionation. *Analytical Chemistry* 1999;71:911–918. [PubMed: 10079757]
- Yang J, Huang Y, Wang XB, Becker FF, Gascoyne PRC. Differential analysis of human leukocytes by dielectrophoretic field-flow-fractionation. *Biophysical Journal* 2000;78:2680–2689. [PubMed: 10777764]
- Zheng, S.; Tai, Y.; Kasdan, H. A Micro Device for Separation of Erythrocytes and Leukocytes in Human Blood. *Proceedings of the 27th Annual International Conference of the Engineering in Medicine and Biology Society* 2005; Shanghai, China. 2005a. p. 1024-1027.
- Zheng, S.; Yung, R.; Tai, Y.; Kasdan, H. Deterministic lateral displacement MEMS device for continuous blood cell separation. *Proceedings of IEEE International Conference on Micro Electro Mechanical Systems (IEEE-MEMS 2005)*; Miami Beach, Florida, USA. 2005b. p. 851-854.

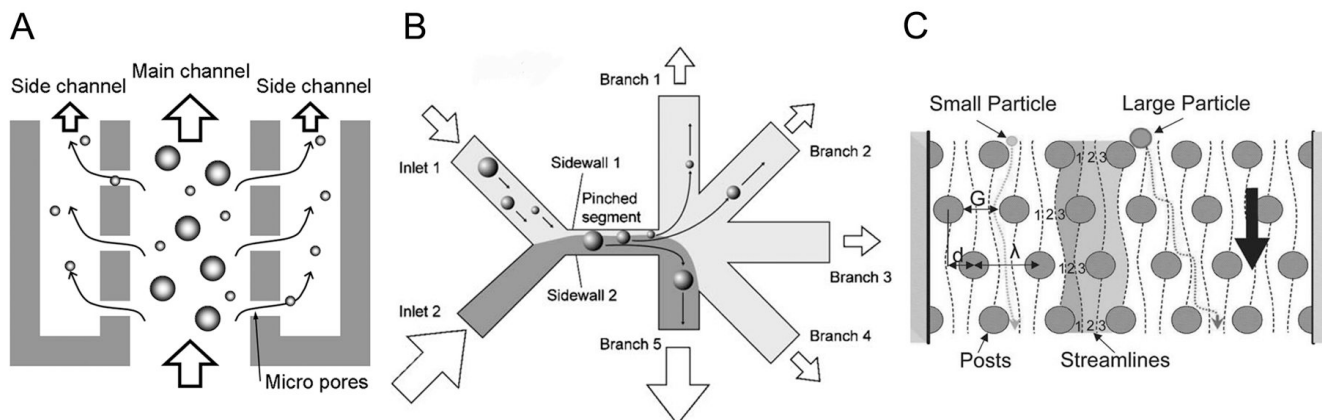


**Figure 1.**

Particle separation with cross flow filtration and laminar flow. (A) Cross flow filtration. Particles smaller than the micro pores on the side walls are continuously extracted into the side channels. The flow in the main channel perpendicular to the micro pores prevents fouling of larger particles on the pores. (B) Asymmetric pinched flow fractionation. Particles introduced from inlet 1 are hydrodynamically aligned against sidewall 1 of the pinched segment, where the centers of mass of the particles are dictated by the radii. Particles are then separated into different trajectories in the diverging section. Reproduced from Takagi et al., 2005 by permission of The Royal Society of Chemistry. (C) Deterministic lateral displacement. In a laminar flow around staggered arrays of posts, small particles stay within a band stream (between two adjacent dashed lines) and come back to the same lateral position every three rows. Large particles, however, are forced to laterally shift after each row as the center of mass needs to cross the boundary of the two adjacent streams. Adapted from Davis et al., 2006, Copyright 2006 National Academy of Sciences, U.S.A.

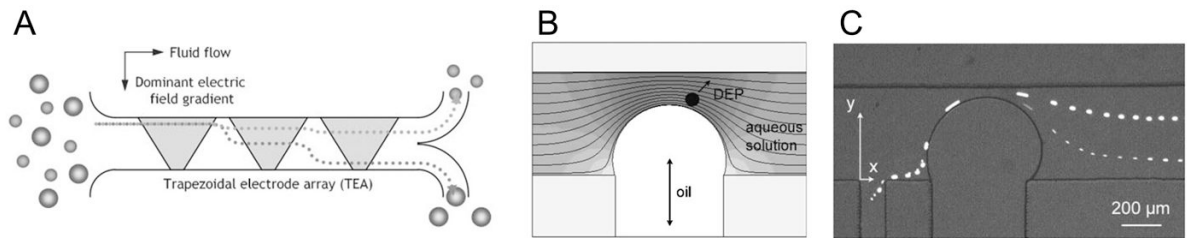


**Figure 2.**

Particle separation by DEP forces. (A) A DEP deflector by the trapezoidal electrode array. Polystyrene beads immersed in a separation buffer experience nDEP force upon encountering each of the trapezoidal electrodes. This nDEP force on the particle is size dependent, resulting in particle fractionation in the transverse direction. Reproduced from Choi and Park, 2005 by permission of The Royal Society of Chemistry. (B) A schematic representation of the electric field strength contours near the oil droplet and the nDEP force on a particle. (C) Superposed trajectories of the 5.7  $\mu\text{m}$  and 15.7  $\mu\text{m}$  particles separated by DC-iDEP. Reproduced from Barbulovic-Nad et al., 2006 by permission of The Royal Society of Chemistry.



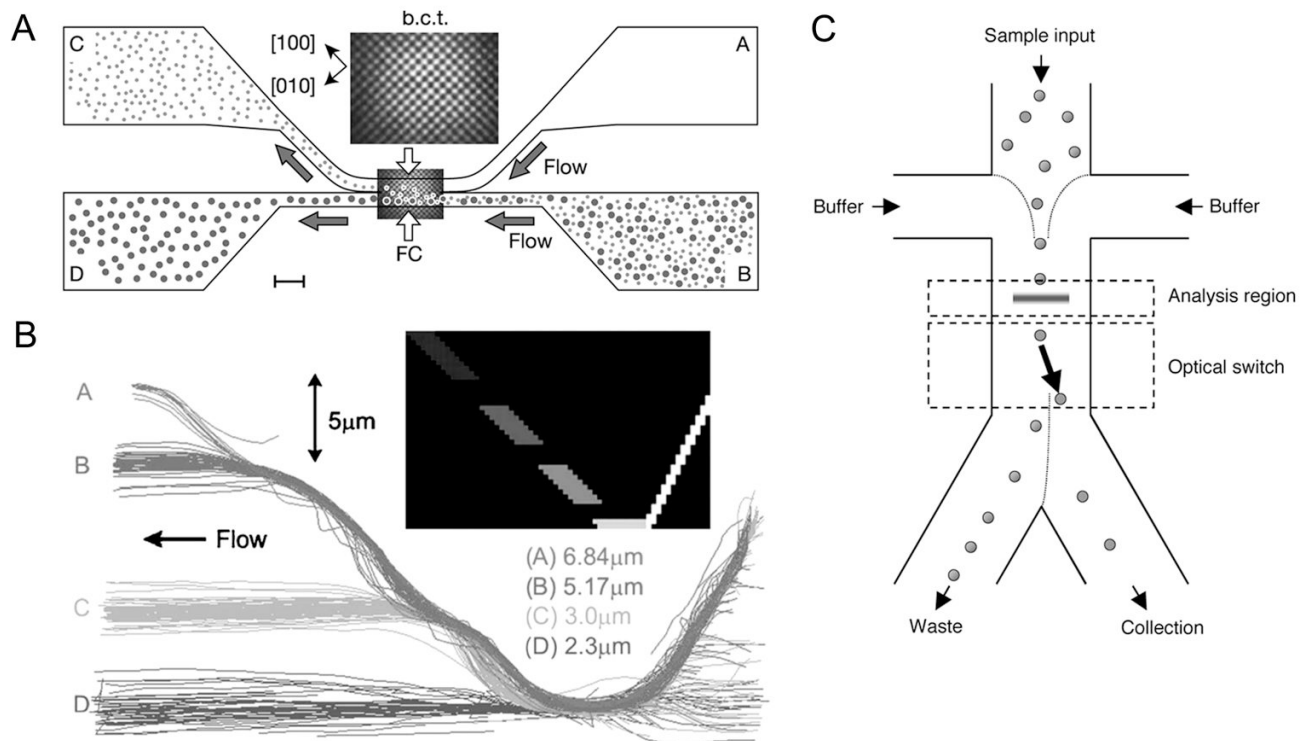


**Figure 3.**

Particle separation by optical forces. (A) Binary fractionation with an optical lattice. A three-dimensional optical lattice formed in the fractionation chamber (FC) exerts the optical gradient force, guiding one species of the particles into the upper flow field. Adapted by permission from Macmillan Publishers Ltd: Nature, MacDonald et al., 2003, copyright 2003. (B) Fractionation of polydisperse particles. The acousto-optically generated optical guide (inset) traps all the particles, then releases them in a size-increasing order, achieving lateral fractionation of four different sizes. Reproduced from Milne et al., 2007 by permission from Optical Society of America, Copyright 2007. (C) A microscale fluorescent activated cell sorter with optical force switching. After being aligned to the center of the channel by flow focusing, cells are analyzed and then switched based on their detected fluorescence. Target cells are directed by the laser to the collection outlet while all the other cells flow to the waste outlet. Adapted by permission from Macmillan Publishers Ltd: Nature Biotechnology, Wang et al., 2005, copyright 2005.

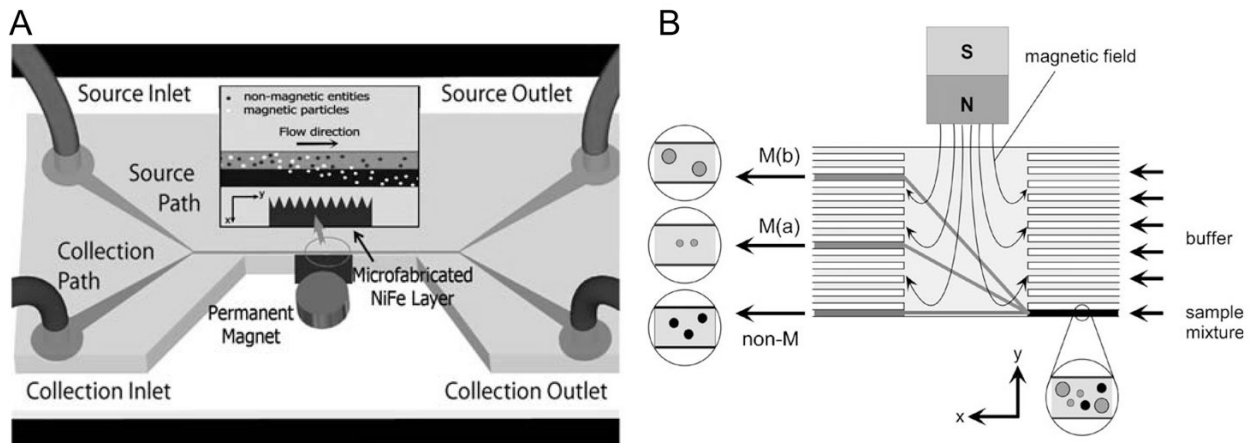


**Figure 4.**

Particle separation by magnetic forces. (A) The two laminar streams, the source stream containing both magnetic and non-magnetic particles and the collection stream without particles, flow through a strong magnetic field gradient produced by the microfabricated NiFe microcomb. Magnetic particles are extracted into the collection stream by magnetic force in the direction perpendicular to the flow. Adapted from Xia et al., 2006, Copyright 2006, with kind permission of Springer Science and Business Media. (B) In free-flow magnetophoresis, particles are laterally fractionated in the separation chamber, then collected into different outlet channels. Reprinted from Pamme et al., 2006, Copyright 2006, with permission from Elsevier.

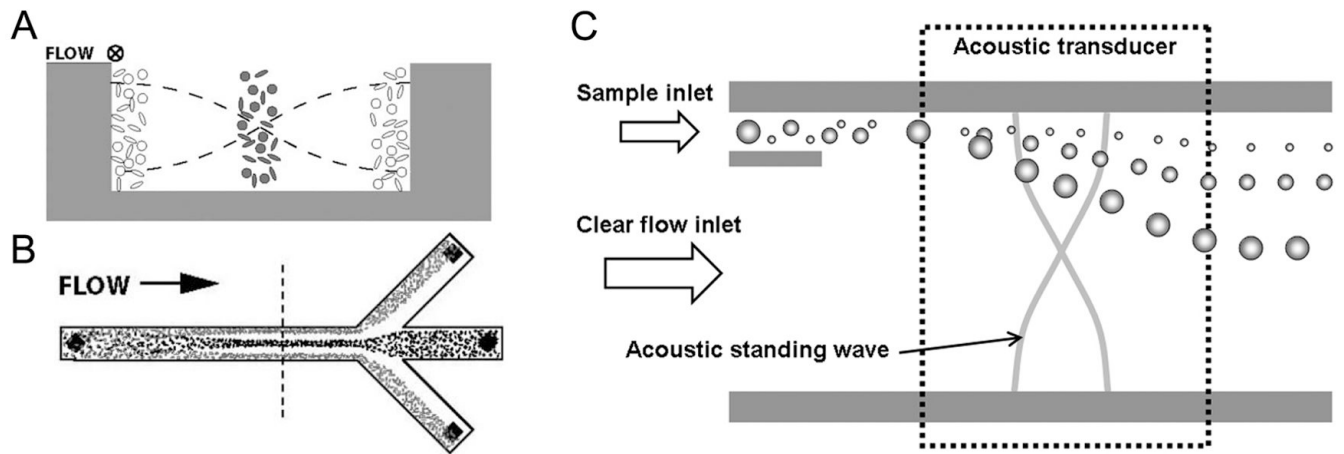


**Figure 5.**

Particle separation by acoustic forces. (A) Two particle types of opposite  $\phi$  are positioned, by the acoustic forces, in the pressure nodal and anti-nodal planes of a standing wave. (B) The top view of a continuous separation of two particle types from each other. Reproduced from Petersson et al., 2004 by permission of The Royal Society of Chemistry. (C) Free-flow acoustophoresis. A stream of mixed particles was fractionated as it passes through the acoustic standing wave section. In this case, the acoustic force differentially deflects particles in a size-dependent manner.

Table 1

List of dielectrophoretic force, magnetic force, and primary radiation force on a spherical particle.

Force type	Formula	Definition of factors
Dielectrophoretic <sup>a</sup>	$\mathbf{F}_{dep} = 2\pi\epsilon_m r^3 \operatorname{Re}[f_{CM}] \nabla  \mathbf{E}_{rms} ^2 \quad (1)$	Clausius-Mossotti factor $f_{CM} = \frac{\epsilon_p^\square - \epsilon_m^\square}{\epsilon_p^\square + 2\epsilon_m^\square}$
Magnetic <sup>b</sup>	$\mathbf{F}_{mag} = \frac{2\pi r^3 (\chi_p - \chi_m)}{3\mu_0} \nabla  \mathbf{B} ^2 \quad (2)$	
Acoustic primary radiation <sup>c</sup>	$F_{PRF} = - \left( \frac{2\pi^2 p_0^2 r^3 \beta_m}{3\lambda} \right) \phi(\beta, \rho) \sin(2kx) \quad (3)$	The acoustic contrast factor $\phi(\beta, \rho) = \frac{5\rho_p - 2\rho_m}{2\rho_p + \rho_m} - \frac{\beta_p}{\beta_m}$

Variables and parameters  
 $r$ : the particle's radius,  $\epsilon_p^\square = \epsilon_p - j(\sigma_p/\omega)$  and  $\epsilon_m^\square = \epsilon_m - j(\sigma_m/\omega)$ : the complex permittivities of the particle and medium, respectively,  $\mathbf{E}_{rms}$ : root-mean-square value of electric field,  $\chi_p$  and  $\chi_m$  magnetic susceptibilities of the (magnetic) particle and medium, respectively,  $\mu_0$ : the permeability,  $\mathbf{B}$ : the magnetic flux density,  $p_0$ : the acoustic pressure amplitude,  $\lambda$ : the wavelength of the acoustic wave,  $k$ : the wave number,  $\beta_p$  and  $\beta_m$ : the compressibilities of the particle and medium, respectively,  $\rho_p$  and  $\rho_m$ : the densities of the particle and medium, respectively.

<sup>a</sup>Jones, 1995,<sup>b</sup>Hatch and Stelter, 2001,<sup>c</sup>Laurell et al., 2007

**Table 2**

List of separation methods based on filtration, laminar flow, dielectrophoretic force, optical gradient force, magnetic force, and acoustic force.

Method	Cross flow filtration	Laminar flow	Dielectrophoresis	Optical force	Magnetic force	Acoustic force
Separation criteria	Size	Size, shape	Size, permittivity	Size, shape, refractive index	Size, susceptibility	Size, density, compressibility
Target sample	Microparticles, cells	Microparticles, cells, DNA	Microparticles, cells	Microparticles, cells	Magnetic particles, magnetically tagged cells	Microparticles, cells
Resolution <sup>a</sup>	RBCs and WBCs <sup>d</sup>	Polystyrene particles (0.5µm and 0.86µm) <sup>f</sup> DNA (61 and 158kb) <sup>g</sup>	Polystyrene particles (4.1µm and 6.0µm) <sup>k</sup>	Protein microcapsules (2µm and 4µm) <sup>o</sup> Silica spheres (2.3µm, 3.0µm, 5.17µm, and 6.84 µm) <sup>p</sup>	Superparamagnetic (1.6µm) and non-magnetic (2µm) particles <sup>s</sup>	Polystyrene particles (2µm, 5µm, 8µm, and 10µm) and platelets, WBCs, and RBCs <sup>v</sup>
Efficiency <sup>b</sup>	98% <sup>d</sup> , 8% (plasma from whole blood) <sup>e</sup>	Up to 100% <sup>f, h</sup>	>95% <sup>k</sup>	96% <sup>o</sup> ~100% (mixture of four particles) <sup>p</sup>	Up to 92% <sup>s</sup>	>95% <sup>w</sup> 62–94% (mixture of four particles) <sup>y</sup>
Throughput	2×10 <sup>3</sup> cells/s <sup>d</sup>	70 particles/s <sup>i</sup>	0.7 cells/s <sup>k</sup> 1.3×10 <sup>5</sup> cells/s <sup>l</sup> 3×10 <sup>7</sup> cells/s <sup>m</sup>	25 particles/s <sup>o</sup> 100 cells/s <sup>q</sup>	1×10 <sup>4</sup> particles/s <sup>s</sup> 470 particles/s <sup>t</sup>	1×10 <sup>5</sup> cells/s <sup>v, w</sup>
Potential sources of lethal and non-lethal effects on cells <sup>c</sup>	Clogging and shear stress <sup>e</sup>	Shear stress <sup>i, j</sup>	Joule heating and electric field <sup>n</sup>	Optical irradiation and temperature increase <sup>r</sup>	Magnetic field <sup>u</sup>	Temperature increase <sup>x</sup>
Instrumentation requirement / portability	Fluidic pumps Highly portable	Fluidic pumps Highly portable	Fluidic pumps, and a function generator (AC-DEF) or DC high voltage supply (DC-DEF) Portable	Fluidic pumps and laser optics Limited portability due to optical setup	Fluidic pumps and a permanent magnet Highly portable	Fluidic pumps, acoustic transducers, and a function generator Portable

<sup>a</sup>Typical examples selected from the literature.

<sup>b</sup>Separation efficiency of binary separation of particles unless otherwise mentioned.

<sup>c</sup>See the text for detail.

<sup>d</sup>VanDelinder and Groisman, 2007.

<sup>e</sup>VanDelinder and Groisman, 2006.

<sup>f</sup>Sai et al., 2006.

<sup>g</sup>Huang et al., 2004.

- <sup>h</sup> Yamada et al., 2004,
- <sup>i</sup> Takagi et al., 2005,
- <sup>j</sup> Ma et al., 2002,
- <sup>k</sup> Krajc et al., 2006,
- <sup>l</sup> Doh and Cho, 2005,
- <sup>m</sup> Hu et al., 2005,
- <sup>n</sup> Voldman, 2006,
- <sup>o</sup> MacDonald et al., 2003,
- <sup>p</sup> Milne et al., 2007,
- <sup>q</sup> Wang et al., 2005,
- <sup>r</sup> Liu et al., 1995; Neuman et al., 1999; Peterman et al., 2003,
- <sup>s</sup> Xia et al., 2006,
- <sup>t</sup> Lin et al., 2007,
- <sup>u</sup> Seidl et al., 1999,
- <sup>v</sup> Petersson et al., 2007,
- <sup>w</sup> Petersson et al., 2004,
- <sup>x</sup> Evander et al., 2007